

INVESTIGATING THE EFFECT OF SLURRY SEAWATER FLOW IN CARBON-STEEL ELBOWS

Mohamed Shehadeh^{1*}, Mohammed Anany² and Ibrahim Hassan³

¹Marine Engineering Dep., Arab Academy for Science, Technology and Maritime
Transport, Alexandria, Egypt.

*Email: ezzfahmy@yahoo.com Phone: +203 5622366

²Mechanical Engineering Dep., Arab Academy for Science, Technology and Maritime
Transport, Alexandria, Egypt.

³Basic & Applied Sciences (Chemical Engineering) Department
Arab Academy for Science, Technology and Maritime Transport, Alexandria, Egypt.

ABSTRACT

Understanding the failure mechanism due to erosion helps in introducing predictive means for parts that are vulnerable to erosion–corrosion effects, such as elbows. This paper is concerned with studying the behavior of steel elbows working in erosive environments. Rates of iron losses due to both flow rate variations and sand concentration variations were investigated. In order to avoid interference from other parts of the system, a PVC test rig, fitted with only one steel elbow at a time, was constructed. The flow rate was controlled to cover both the laminar and turbulent flow regimes. The sand concentration varied from nil up to 9 grams per liter. A spectrophotometer was utilized to measure the quantity of iron losses. Results showed that the critical sand concentration for the erosion mechanism is 3 g/l. Also an empirical formula was developed for estimating the erosion–corrosion rate in laminar and turbulent flow regimes with different sand contamination levels.

Keywords: slurry seawater, erosion–corrosion, laminar flow, turbulent flow.

INTRODUCTION

Seawater systems (i.e. pipelines, elbows) are used by many industries, such as onshore/offshore oil and gas production, power plants, and coastal industrial plants (Antaki, 2003; Yang & Cheng, 2012). The main use of seawater is for cooling purposes, but it is also used for fire-fighting, oilfield water injection, and desalination plants (Kehr, 2003). (Nayyar, 2000) describes pipeline networks as the arteries and veins of modern civilization. Pipeline networks are implemented for fluid transmission and cooling purposes in both onshore and offshore applications. The widespread use of pipeline networks and their vast application in the oil and gas industries, such as for crude oil and natural gas transportation from production fields to refineries, processing plants and distribution to consumers, explain the necessity for continuous monitoring and diagnosis of pipeline networks (Cronin, 2001) in order to avoid catastrophic failures that can have grave environmental effects. Many studies have also discussed the costly terms of production losses especially due to pipeline corrosion damage (Kehr, 2003; Roberge, 2000; Winkelmanns & Wevers, 2003; Yang & Cheng, 2012). Several structural and mechanical elements, such as elbows in pipeline networks and ships' propellers churning in the ocean, can suffer from erosion–corrosion problems. Erosion–corrosion, also known as flow-assisted corrosion, is the general term encompassing a

spectrum of mechanisms, from accelerated corrosion to purely mechanical damage, which cause high rates of material loss in industries (Chen, 2006; Roberge, 2000; Sanjuan, 2008; Yusof, Jamaludin, Abdullah, Hanafi, & Zain, 2012). In the former, moving liquid particles cause the damage, whereas collapsing (unstable) vapor bubbles induce surface damage in the latter (Charde, 2012; Roberge, 2000). Fontana (1986) defines erosion as the acceleration or increase in the rate of deterioration or attack on a metal because of the relative movement between a corrosive fluid and the metal surface. Generally, this movement is quite rapid, and mechanical wear effects or abrasion are involved. Erosion results in the gradual removal of the surface layer in the form of small chippings (Chen, 2006). Erosion–corrosion is characterized in appearance by grooves, gullies, waves, or rounded holes and usually exhibits a directional pattern (Fontana, 1986). The motion is usually one of high velocity, with mechanical wear and abrasion effects (Antaki, 2003). Flow velocities influence the erosion behavior, so when the velocity of the flow increases the rate of erosion–corrosion increases (Roberge, 2000; Yang & Cheng, 2012).

The materials selection process plays an important role in minimizing the erosion–corrosion damage. Several environmental modifications can be implemented to minimize the risk of erosion failures (Hu & Neville, 2009; Nayyar, 2000; Ridha, Fonna, Huzni, Supardi, & Ariffin, 2013; Sundararajan, 1991). For example, (Shedadeh, Hassan, Mourad, & El-Gamal, 2012) demonstrated that the detection of erosion enhances the overall system reliability and safety, as well as the system performance. They implemented acoustic emission techniques for monitoring pipeline networks in order to accommodate the early detection of any abnormal behavior of the system. However, the erosion–corrosion behavior is affected by many parameters such as the flow velocity (Yang & Cheng, 2012) and the solid-particle contaminant concentration (Ansari, Mohammadi, & Oskouei, 2012). The flow velocity is widely studied because of its influence on the design process of fresh/sea water systems subjected to corrosion effects (Ansari et al., 2012; Hu & Neville, 2009; Roberge, 2000; Yang & Cheng, 2012). The erosion–corrosion rate is estimated from the quantity of iron loss from the carbon steel of the pipeline system. The erosion–corrosion rate is given by the following expression:

$$\text{Erosion - corrosion rate} = \frac{WL}{A \times T} \quad (.1)$$

where WL = iron loss weight (mg)
 A = elbow surface area (m²)
 T = time (min)

In the present paper, a series of laboratory experiments is carried out to study the behavior of erosion–corrosion in carbon steel elbows. The elbows are connected to a plastic pipeline system filled with seawater contaminated with sand at three different concentrations and running at various flow velocities covering the laminar and turbulent flow regimes.

microprocessor-controlled, single-beam instrument for colorimetric testing in the laboratory or the field. This is used to measure the quantity of iron loss from the elbow in each sample of seawater. Also ferrower iron reagent was used to determine the quantity of iron in the seawater. The erosion–corrosion analyses in these experiments were carried out to determine its rate in each elbow in the four different mediums by changing the velocity of the flow every hour. A water sample of the out-flowing water was collected every 20 minutes in a clean test tube which was initially washed with distilled water. Four elbows were tested in four different mediums (i.e. seawater and three sand concentrations). In order to study the corrosion effect, a series of experiments was carried out with seawater only. Thereafter, to study the erosion effect, 3 g/l, 6 g/l and 9 g/l of sand particles were added to the seawater to obtain various effects of erosive environments that will predict the behavior of the erosion–corrosion rate in steel elbows. Three velocities for the laminar state (Re 582, 1176 and 2148), and four velocities for the turbulent state (Re 7878, 13107, 19296 and 25922) were investigated, as shown in Table 1.

Table 1. Erosion–corrosion rate calculations.

| Test # | Flow Regime | Re | Time (min) | Seawater (mg/m ² min) | 3 g/l sand (mg/m ² min) | 6 g/l sand (mg/m ² min) | 9 g/l sand (mg/m ² min) |
|--------|-------------|-------|------------|----------------------------------|------------------------------------|------------------------------------|------------------------------------|
| 1 | Laminar | 582 | 20 | 0.022 | 0.049 | 0.076 | 0.087 |
| | | | 40 | 0.026 | 0.050 | 0.079 | 0.087 |
| | | | 60 | 0.027 | 0.050 | 0.079 | 0.088 |
| 2 | Laminar | 1176 | 20 | 0.036 | 0.060 | 0.084 | 0.091 |
| | | | 40 | 0.040 | 0.062 | 0.083 | 0.093 |
| | | | 60 | 0.044 | 0.063 | 0.084 | 0.096 |
| 3 | Laminar | 2148 | 20 | 0.053 | 0.071 | 0.087 | 0.098 |
| | | | 40 | 0.052 | 0.070 | 0.090 | 0.100 |
| | | | 60 | 0.054 | 0.072 | 0.090 | 0.101 |
| 4 | Turbulent | 7878 | 20 | 0.093 | 0.204 | 0.218 | 0.400 |
| | | | 40 | 0.090 | 0.211 | 0.231 | 0.433 |
| | | | 60 | 0.095 | 0.212 | 0.258 | 0.474 |
| 5 | Turbulent | 13107 | 20 | 0.118 | 0.313 | 0.467 | 0.711 |
| | | | 40 | 0.121 | 0.357 | 0.500 | 0.722 |
| | | | 60 | 0.122 | 0.393 | 0.541 | 0.748 |
| 6 | Turbulent | 19296 | 20 | 0.129 | 0.400 | 0.578 | 0.933 |
| | | | 40 | 0.132 | 0.433 | 0.600 | 0.978 |
| | | | 60 | 0.135 | 0.459 | 0.630 | 0.993 |
| 7 | Turbulent | 25922 | 20 | 0.151 | 0.711 | 0.800 | 1.178 |
| | | | 40 | 0.151 | 0.756 | 0.833 | 1.211 |
| | | | 60 | 0.152 | 0.778 | 0.881 | 1.252 |

RESULTS AND DISCUSSION

Iron Weight Losses

Total weight loss tests were carried out on the carbon steel without the flow-induced solid particles (i.e. corrosion condition) and afterwards at three different solid-particle concentrations in order to study the performance of carbon steel materials in erosive–

corrosive mediums. Accordingly, the appropriate material loss models can be used in their range of applicability. The total weight loss of iron was measured for 40 minutes of operation of seawater, as well as the weight loss for sand-contaminated seawater with sand concentrations of 3 g/l, 6 g/l and 9 g/l at different flow velocities. Iron weight losses in the case of uncontaminated seawater can be attributed to corrosion mechanisms. However, the increase in weight losses due to sand contamination is the result of erosion effects. This approach is similar to that described by (Ansari et al., 2012). Figure 2 illustrates the normalized weight loss of iron against the flow velocity. For the turbulent flow regime, a significant increase in the weight loss is observed as the flow velocity is increased. Such behavior was not observed in the laminar regime. Hence, it can be concluded that the flow velocity has no significant effect on erosion rates, but only the sand concentration. On the other hand, in the turbulent flow all of the sand concentrations as well as the flow velocity have a significant effect on erosion. Data given in Figure 2 can be expressed as follows:

$$\ln\left(\frac{C}{C_0}\right)_{Fe} = a_1 \ln Re + a_2 \tag{2}$$

where C_0 is the initial iron concentration in the water used for the experiment, which was found to be equal to $4 \times 10^{-3} \text{ mg/l}$, and C is the iron concentration due to the erosion–corrosion effects. The coefficients of Eq. (2) are listed in Table 2.

Table 2. Coefficients of Eq. (2).

| Flow regime | a_1 | a_2 |
|-------------------------------------|------------------------------------|------------------------------------|
| Uncontaminated seawater (laminar) | 0.550 | -1.735 |
| Uncontaminated seawater (turbulent) | 0.420 | -0.735 |
| Contaminated seawater (laminar) | $0.009C_s^2 - 0.137 C_s + 0.586$ | $-0.078 C_s^2 + 1.190 C_s - 2.085$ |
| Contaminated seawater (turbulent) | $-0.011 C_s^2 + 0.114 C_s + 0.759$ | $0.123 C_s^2 - 1.155 C_s - 2.779$ |

where C_s is the sand concentration in grams per liter.

Estimation of Erosion–Corrosion Rate

Analysis techniques are developed here to extract significant features of the erosion–corrosion rate. Hence, the erosion–corrosion rate was calculated using Eq. (Chandra, Singh, & Gupta) in all mediums for seven different velocities (i.e. Reynolds number) with 20 minute increments (see Table 1). Figure 3 shows the erosion–corrosion rate of iron losses and individual contributors as a function of the sand concentration and Reynolds number. Figure 3(a) shows a linear relationship between the erosion–corrosion rate and the velocity for the flow for the laminar case with constant time after 40 minutes of operation in each velocity. Figure 3(b) shows the same relation for the turbulent flow case. From the observation of the trends in all mediums, it is clear that the increase of the erosion–corrosion rate is very high due to the change in the flow regime from laminar to turbulent, especially for seawater with 9 g/l of sand in turbulent

flow. However, for non-contaminated seawater, the increase of the erosion–corrosion rate in turbulent flow is low, as shown in Figure 3(b). The results here agree with other researchers e.g. (Ansari et al., 2012; Hu & Neville, 2009; Yang & Cheng, 2012). They proved that the erosion–corrosion rate increases directly as the impact velocity of the particles increases.

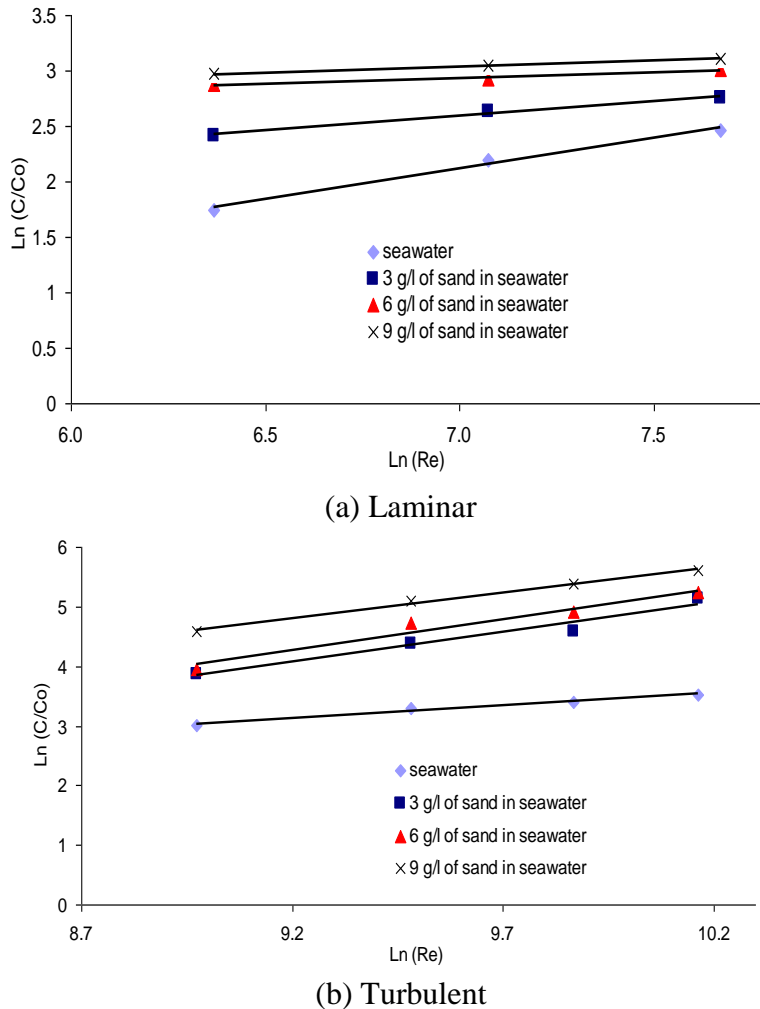


Figure 2. Normalized weight losses vs Reynolds number at time 40 minutes.

Figure 3 clearly indicates the great increase in the erosion–corrosion rate caused by increasing the quantity of solid particles in seawater in both laminar and turbulent flow. The erosion–corrosion rate obeys a linear relationship with the different flow regimes. The following equations for weight loss rates are proposed from the observed linear trends of Figure 3:

$$\text{Erosion–corrosion rate} = b_1 \text{Re} + b_2 \tag{3}$$

where b_1 and b_2 are given in Table 3 and C_s is the sand concentration in grams per liter. The equations can help in the prediction of the erosion–corrosion rates based on the

flow regime and solid particle concentrations for the range of the studied flow velocities.

Table 3. Coefficients of Eq. (3).

| Flow regime | b_1 | b_2 |
|-------------------------------------|---|--|
| Uncontaminated seawater (laminar) | 2×10^{-5} | 0.016 |
| Uncontaminated seawater (turbulent) | 3×10^{-6} | 0.730 |
| Contaminated seawater (laminar) | $(2C_s^2 - 30C_s + 200) \times 10^{-7}$ | $(-C_s^2 + 21C_s - 10) \times 10^{-3}$ |
| Contaminated seawater (turbulent) | $(6C_s^2 - 5C_s + 4) \times 10^{-7}$ | $(2C_s^2 - 5C_s - 41) \times 10^{-3}$ |

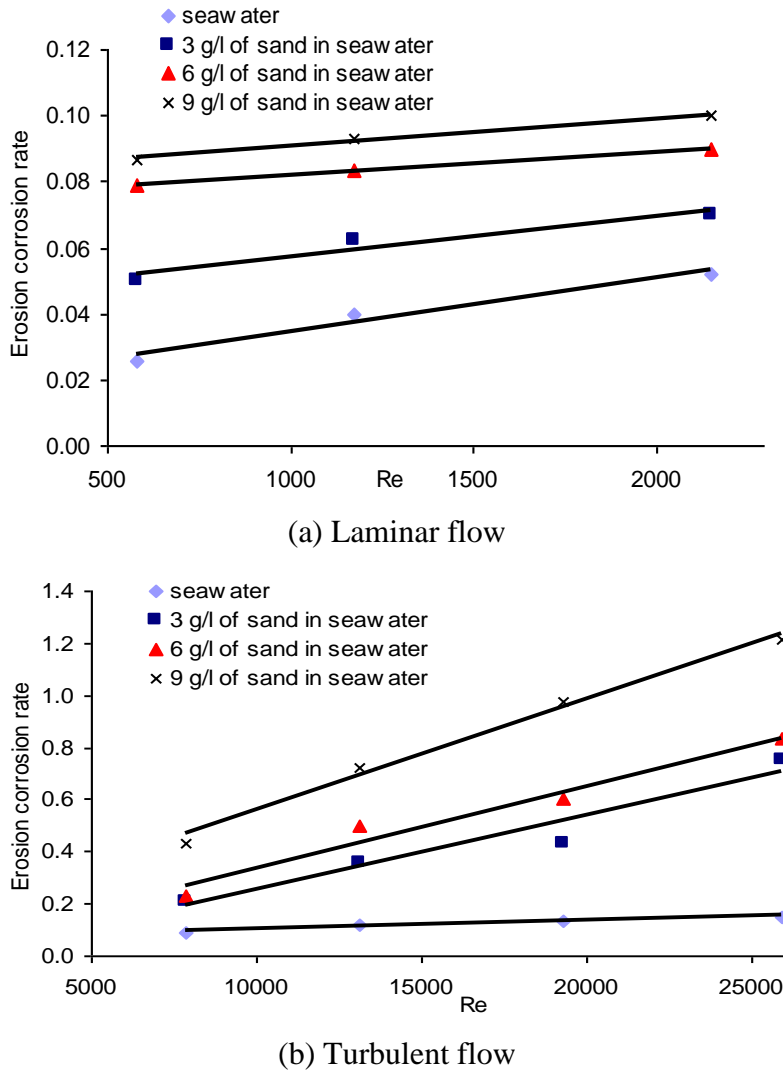


Figure 3. Erosion–corrosion rate vs Reynolds number.

Internal Surface Condition

To predict the condition of the internal surface of the elbow due to fluid containing solid particles, it is important to determine the conditions where erosion–corrosion becomes the dominant degradation process rather than flow-induced corrosion. A high-resolution camera was used to study the shape of the internal surface after seven hours of operation for each sand concentration. The erosion of the elbows is depicted in Figure 4. For pure seawater and 3 g/l sand (Figures 4 a and b) corrosion is more evident than erosion, whereas for sand concentrations of 6 g/l and 9 g/l traces of erosion are more obvious (Figures 4 c and d). Hence, erosion effects were obvious for sand concentrations greater than 3 g/l of sand in this type of elbow. This is because the increase in erosion rate with velocity is associated with the increase in kinetic energy of the erodent and the number of sand impacts per unit time, causing greater damage to the elbow’s metal surface. Since solid particles possess more inertia forces in comparison to seawater, they tend to fail to change their direction of motion within the elbow and hence hit the outer bend side of the elbow. Hence, most of the erosion was observed to take place at this outer bend of the elbow, which is in accordance with the work of (Keating & Nesic, 1999) and (Ansari et al., 2012).

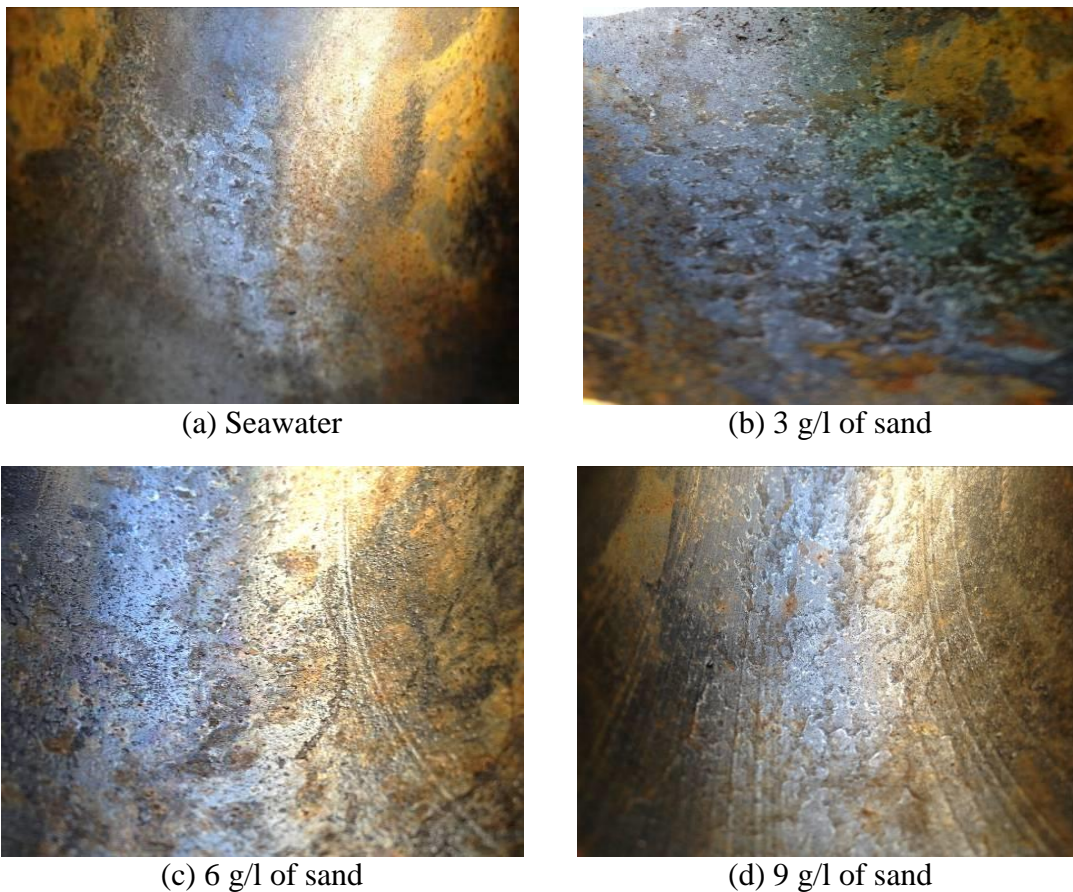


Figure 4. Internal elbow surface after seven hours of operation in different sand concentrations

CONCLUSIONS

In this research the effect of seawater flow rate and seawater contamination level on erosion–corrosion rates was investigated. Four carbon steel elbows were tested at different sand contamination levels. The experiments were run to include both laminar and turbulent flow regimes. The results showed that the rates of erosion increase linearly with the increase of flow velocities and sand contamination levels. Also, it was found that 3 g/l of sand is a critical concentration at which erosion mechanisms are observed. The erosion rate was doubled on the transition from the laminar to the turbulent flow regime, whereas it increased fourfold for seawater containing 9 g/l of sand when the flow regime changed into a turbulent one. The study proposes a linear equation for predicting the erosion–corrosion rate with two sets of coefficients for both the laminar and turbulent flow regimes. These proposed empirical formulas could help in predicting erosion rates and in the pipeline design process. Finally, further investigation on different amounts of sand concentrations, solid particle sizes and material types needs to be carried out.

REFERENCES

- Ansari, M., Mohammadi, S., & Oskouei, M. K. (2012). Two-phase gas/liquid-solid flow modelling in 90° bends and its effect on erosion. *Global Journal of Researches In Engineering*, 12(1), 35-44.
- Antaki, G. A. (2003). *Piping and pipeline engineering* (3rd ed. ed.). USA: Taylor and Francis.
- Chandra, R., Singh, S. P., & Gupta, K. (1999). Damping studies in fiber-reinforced composites—a review. *Composite structures*, 46(1), 41-51.
- Charde, N. (2012). Effects of electrode deformation on 304 austenitic stainless steel weld geometry of resistance spot welding. *Journal of Mechanical Engineering and Sciences*, 3, 261-270.
- Chen, C. (2006). *Interaction of chemical and mechanical effects in erosion-corrosion of pipeline steels in oil sand wastewater transportation*. University of Alberta.
- Cronin, D. S. (2001). *Assessment of corrosion defects in pipelines*: University of Waterloo.
- Culkin, F. (1965). The major constituents of sea water. *Chemical oceanography*, 1, 121-161.
- Fontana, M. G. (1986). *Corrosion engineering*: Tata McGraw-Hill Education.
- Guo, C., Zhang, C., & Païdoussis, M. (2010). Modification of equation of motion of fluid-conveying pipe for laminar and turbulent flow profiles. *Journal of Fluids and Structures*, 26(5), 793-803.
- Hu, X., & Neville, A. (2009). Co2 erosion–corrosion of pipeline steel (api x65) in oil and gas conditions—a systematic approach. *Wear*, 267(11), 2027-2032.
- Keating, A., & Nesic, S. (1999). *Prediction of two-phase erosion-corrosion in bends*. Paper presented at the Second International Conference on CFD in the Minerals and Process Industries, CSIRO, Melbourne, Australia.
- Kehr, J. A. (2003). Fusion-bonded epoxy internal linings and external coatings for pipeline corrosion protection. In Nayyar, M. L. (Ed.), *Piping handbook (7th ed.)*. USA: McGraw-Hill.
- Nayyar, M. (2000). *Piping handbook*: McGraw-Hill.

- Ridha, M., Fonna, S., Huzni, S., Supardi, J., & Ariffin, A. K. (2013). Atmospheric corrosion of structural steels exposed into the 2004 tsunami affected areas in aceh. *International Journal of Automotive and Mechanical Engineering*, 7, 1015-1023.
- Roberge, P. R. (2000). *Handbook of corrosion engineering* (Vol. 1128): McGraw-Hill New York.
- Sanjuan, E. (2008). 'Studies of corrosion and stress corrosion cracking behavior of high-strength pipeline steels in carbonate/bicarbonate solutions. *Master of Science Degree Thesis, University of Calgary.*
- Shedadeh, M., Hassan, I., Mourad, H., & El-Gamal, H. (2012). *Monitoring erosion–corrosion in carbon steel elbow using acoustic emission technique.* Paper presented at the 30th European Conference on Acoustic Emission Testing / 7th International Conference on Acoustic Emission, Granada, Spain.
- Sundararajan, G. (1991). A comprehensive model for the solid particle erosion of ductile materials. *Wear*, 149(1), 111-127.
- Winkelmans, M., & Wevers, M. (2003). Non-destructive testing for corrosion monitoring in chemical plants. *Journal of Acoustic Emission*, 20, 206-217.
- Yang, Y., & Cheng, Y. (2012). Parametric effects on the erosion–corrosion rate and mechanism of carbon steel pipes in oil sands slurry. *Wear*, 276, 141-148.
- Yusof, M. F. M., Jamaludin, N., Abdullah, S., Hanafi, Z. H., & Zain, M. S. M. (2012). Monitoring and assessment of acoustic emission signatures during fatigue mechanism of api5lx70 gas pipeline steel. *Journal of Mechanical Engineering and Sciences*, 2, 237-250.